Synthesis, photolysis studies and *in vitro* photorelease of caged TRPV1 agonists and antagonists†

Michael P. Van Ryssen,[a] Nicolaos Avlonitis,[a] Rashid Giniatullin,[b] Craig McDougall,[c] James L. Carr,[a] Megan N. Stanton-Humphreys,[a,d] Emma L. A. Borgström,[a] C. Tom A. Brown,[c] Dmitriy Fayuk,[b] Alexander Surin,[e] Minna Niittykoski,[e] Leonard Khiroug[e] and Stuart J. Conway*[d]

Received 23rd July 2009, Accepted 24th August 2009
First published as an Advance Article on the web 24th September 2009
DOI: 10.1039/b914981c

The synthesis of a range of caged TRPV1 agonists and antagonists is reported. The photolysis characteristics of these compounds, when irradiated with a 355 nm laser, have been studied and in all cases the desired compound was produced. Photolysis of a caged TRPV1 agonist in cultured trigeminal neurons produced responses that were consistent with the activation of TRPV1 receptors.

Introduction

Capsaicin (**1**, Fig. 1), the main pungent component of chilli peppers, has long been known to produce a painful irritant effect if injected into the skin, applied to sensitive structures such as the cornea, or tasted.[1–3] In 1997 David Julius and co-workers isolated and cloned the molecular target of capsaicin.[4] They demonstrated that this protein, named transient receptor potential vanilloid subtype 1 (TRPV1), is a non-selective cation channel that is activated by capsaicin, heat above ~45 °C and pH below ~5.5. TRPV1 is found on sensory neurones and hence is involved in nociception;[2] it is also involved in urinary urge incontinence, chronic cough and irritable bowel syndrome.[5] Consequently, there has been great interest in the development of TRPV1 agonists and more significantly antagonists, as drugs for the treatment of these indications and there are a number of TRPV1 antagonists currently in clinical trials.[1,5–8] The biology underpinning the mechanism of action of these compounds, including the location of the ligand-binding site or sites and whether the receptors exist functionally as homomeric or heteromeric tetramers is not fully understood.[1] TRPV1-mediated signalling is further complicated by the discovery that anandamide, an endogenous cannabinoid receptor agonist also functions as an endogenous TRPV1 agonist—an endovanilloid.[1] Therefore, chemical probes that are able to interact selectively with TRPV1 are important for the study of these channels. It would be particularly useful if compounds that can be released in a temporally and spatially controlled manner could be provided.

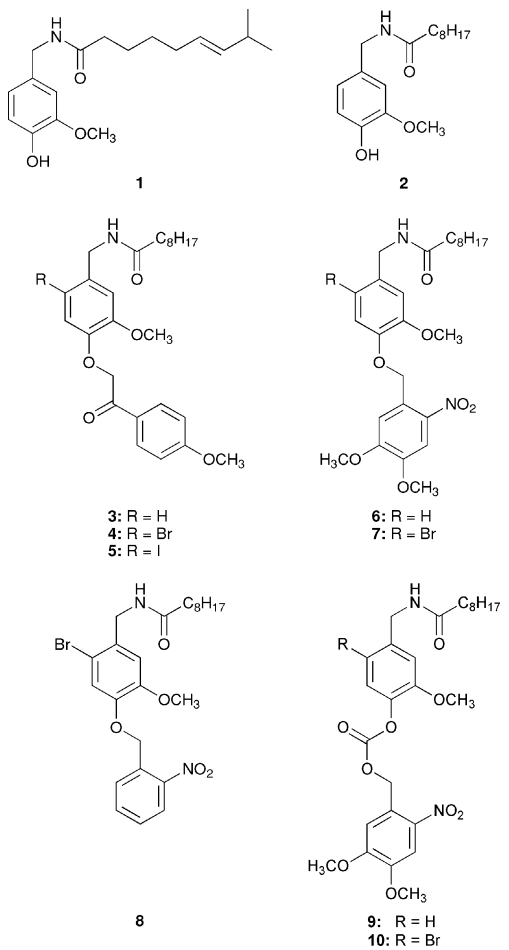

Fig. 1 The structures of capsaicin (**1**), nonivamide (**2**) and the caged TRPV1 ligands that have been synthesised (**3–10**).

One way in which temporal and spatial control can be gained over the release of a biologically active compound is the use of a photolabile protecting group, a process known as caging.[9,10] The photolabile protecting group is attached to the ligand so as to render it biologically inactive. The inactive compound is then introduced into the system under study. Subsequent photolysis

[a]*EaStCHEM and School of Chemistry, Centre for Biomolecular Sciences, University of St Andrews, North Haugh, St Andrews, Fife KY16 9ST, UK*
[b]*Department of Neurobiology, A. I. Virtanen Institute for Molecular Sciences, PO Box 1627, Neulaniementie 2, FIN-70211, Kuopio, Finland*
[c]*SUPA, School of Physics and Astronomy, University of St Andrews, North Haugh, St Andrews, Fife KY16 9SS, UK*
[d]*Department of Chemistry, Chemistry Research Laboratory, University of Oxford, Mansfield Road, Oxford, OX1 3TA, UK. E-mail: stuart.conway@chem.ox.ac.uk; Fax: +44 (0) 1865 285002; Tel: +44 (0) 1865 285109*
[e]*Neuroscience Center, University of Helsinki, Viikinkaari 4, FIN-00014, Helsinki, Finland*

† Electronic supplementary information (ESI) available: General experimental methods; NMR and UV/vis spectra. See DOI: 10.1039/b914981c

releases the active molecule and hence leads to activation of the biological target. The use of caged compounds to allow temporal and spatial control over receptor activation or inactivation has frequently proved invaluable in the study of receptor function.[9–12] There have been a number of caged TRPV1 agonists reported. Miesenbock *et al.* were the first to report a 2-nitro-4,5-(dimethoxy)benzyl (DMNB)-caged derivative of capsaicin, which was used in their studies of photochemical ion channel gating.[13] Katritzky reported some photolysis studies on a biologically inactive DMNB-caged capsaicin derivative.[14] Subsequently, we reported the 4′-(methoxy)phenacyl and DMNB-caged TRPV1 agonists **3** and **6** (Fig. 1), and demonstrated the photorelease of **6** in dorsal root ganglion neurons.[15] At a similar time, Kao reported a number of caged TRPV1 agonists, interestingly demonstrating that attachment of the caging group to the amide nitrogen also produces inactive compounds, which could be photoreleased to yield a TRPV1 agonist.[16] Hagen and co-workers have reported the caging of capsaicin with polar 4,5-dimethoxy-2-nitrobenzyl (DMNB)- and coumarin-derived groups that showed enhanced solubility in aqueous media and the possibility of 2-photon photolysis.[17,18] Herein, we report full synthetic details for our previously reported 4-(methoxy)phenacyl- (**3**) and DMNB-caged (**6**) TRPV1 agonists[15] and the synthesis of a further TRPV1 agonist (**9**) that is linked to the DMNB group *via* a carbonate moiety. In addition, a range of caged TRPV1 antagonists (**4**, **5**, **7**, **8**, **10**) is reported. To the best of our knowledge, these are the first reported caged TRPV1 antagonists. The different caging groups that have been employed potentially instil differential photolysis and physical properties (such as solubility) in the resulting compounds, and hence certain caged compounds may be more applicable in a given setting. The photolysis characteristics of these compounds have been studied and the *in vitro* photolysis of compound **6** is demonstrated.

Results and discussion

Synthetic chemistry

The caged TRPV1 agonists we have developed are based on the structure of nonivamide (**2**). This compound is synthetically simpler to produce than capsaicin and has very similar pharmacological activity.[19–21] Walpole *et al.* have demonstrated that alkylation of the phenol contained within the vanilloid moiety of capsaicin rendered the molecule biologically inactive.[19] Therefore, addition of the caging group to the phenol was considered to be optimal from both a synthetic and a biological standpoint. As only caged TRPV1 agonists have been reported, we were interested in the development of caged TRPV1 antagonists, which would allow inactivation of TRPV1 with spatial and temporal control. As the TRPV1 agonists that we had previously developed were based on the nonivamide scaffold, it seemed logical to employ antagonists with similar structures. Subsequent to the discovery that 5-iodoresiniveratoxin behaves as a TRPV1 antagonist,[22] Appendino and co-workers demonstrated that halogenation of nonivamide also affords TRPV1 antagonists, therefore we have based the synthesis of our caged antagonists on these compounds.[23,24]

Our initial studies employed the 4-methoxyphenacyl caging group,[25] as the side-products produced upon photolysis are less reactive within a biological system than those produced by other common caging groups. We have subsequently broadened the range of caging groups employed to include the 4,5-dimethoxy-2-nitrobenzyl (DMNB) group, the DMNB group linked *via* a carbonate to the phenol, and the 2-nitrobenzyl group. These groups allow us to obtain caged compounds with a range of physical and photolysis characteristics.

A synthetic route that readily affords both the halogenated and unhalogenated nonivamide derivatives was developed (Scheme 1). The commercially available benzonitrile **11** was protected with a TIPS group, both to reduce the risk of the phenol reacting with nonanoyl chloride and also to assist with the selectivity in the halogenation process. The nitrile **12** was reduced to the corresponding benzylamine (**13**) by treatment with $LiAlH_4$. This polar amine (**13**) was used without further purification and treated with nonanoyl chloride to afford the protected TRPV1 agonist **14**, which was reacted with TBAF to afford the TRPV1 agonist, nonivamide, **2**.

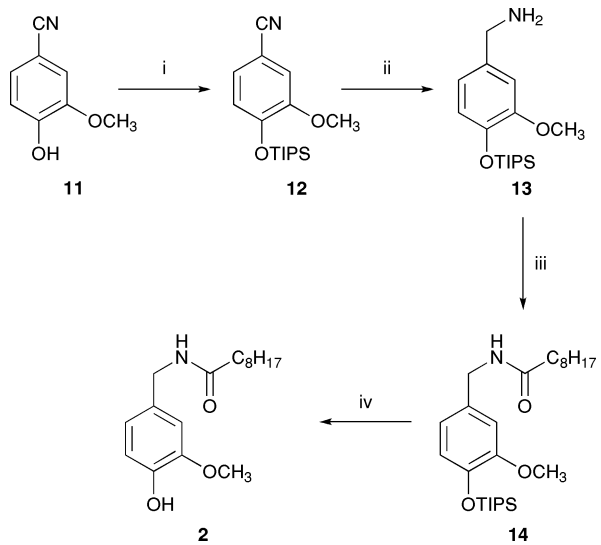

Scheme 1 Synthesis of the TRPV1 agonist, nonivamide, **2**. Reagents and conditions: i. TIPSCl, imidazole, DMF, rt, 91%; ii. $LiAlH_4$, THF, rt, 89% crude yield; iii. nonanoyl chloride, 4-DMAP, pyridine, CH_2Cl_2, 0 °C → rt, 78%; iv. TBAF, THF, rt, 84%.

In order to synthesise the caged TRPV1 antagonists, it was necessary to halogenate the phenyl ring at the 6-positon. Bromination of the TIPS ether **14** was readily achieved by treatment with bromine in dichloromethane at −78 °C (Scheme 2). The low temperature was required in order to obtain the desired regiochemistry in the product (**15**). Execution of the reaction at higher temperature led to a mixture of brominated products. Iodine, in the presence of silver trifluoroacetate and sodium bicarbonate, effected iodination of the TIPS ether **14** to afford **16**. In both cases, the TIPS protecting group was removed by treatment with TBAF in THF at rt furnishing the TRPV1 antagonists **17** and **18**.

The 4-(methoxy)phenacyl caging group was coupled to the phenolic oxygen by treatment of the phenol with sodium hydride in DMF followed by 2-bromo-4′methoxyacetophenone (Scheme 3). In the case of the unhalogenated phenol, the reaction proceeded smoothly in good yield. In the case of both the brominated and iodinated phenols the reaction afforded the desired product in

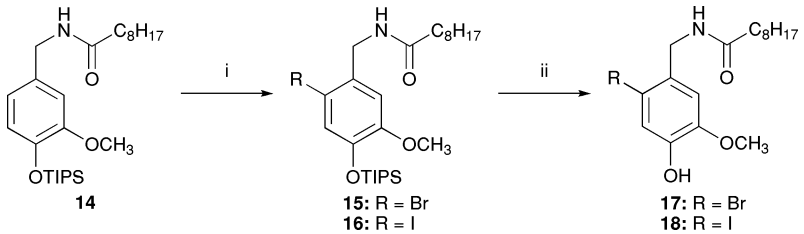

Scheme 2 The bromination or iodination of the TIPS ether **14** to give the TRPV1 antagonists **17** and **18**. Reagents and conditions: R = Br: i. Br_2, CH_2Cl_2, −78 °C, 73%; ii. TBAF, THF, rt, 86%. R = I: i. I_2, $Ag(OCOCF_3)$, Na_2HCO_3, CH_2Cl_2, −10 °C → rt, 49%; ii. TBAF, THF, rt, 66%.

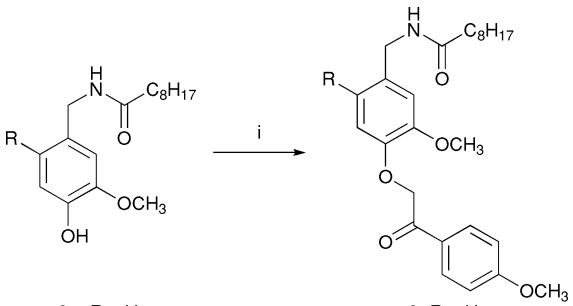

Scheme 3 Protection of the TRPV1 ligands **2**, **17** and **18** with the 4-(methoxy)phenacyl caging groups. Reagents and conditions: R = H: i. NaH, 2-bromo-4′-methoxyacetophenone, DMF, 0 °C → rt, 71%. R = Br: i. NaH, 2-bromo-4′-methoxyacetophenone, DMF, 0 °C → rt, 31%. R = I: i. NaH, 2-bromo-4′-methoxyacetophenone, DMF, 0 °C → rt, 33%.

lower yield, under the same conditions. We attribute the lower yield in these cases to the electronic properties of the halogen atom, which stabilises the negative charge of the generated phenolate anion and reduces its nucleophilicity. We have yet to optimise these reaction conditions, but feel that higher yields in the reactions should be possible.

Addition of the DMNB caging group to the unhalogenated phenol **2** and the brominated phenol **17** was achieved by treatment of the phenol with potassium *tert*-butoxide and 4,5-dimethoxy-2-nitrobenzyl bromide (Scheme 4), affording the caged TRPV1 ligands **6** and **7**. A number of alternative conditions were investigated, including sodium hydride in DMF, but none was found to be as effective as those ultimately employed.

The brominated phenol **17** was coupled to the 2-nitrobenzyl caging group using potassium *tert*-butoxide and 2-nitrobenzyl bromide (Scheme 5), furnishing the caged TRPV1 antagonist **8**. The low yield for this reaction can again probably be attributed to the low nucleophilicity of the brominated phenolate anion.

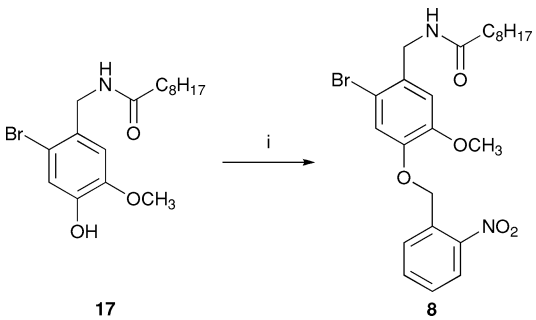

Scheme 5 Protection of TRPV1 antagonist **17** with the 2-nitrobenzyl caging group. Reagents and conditions: i. ^{t}BuOK, 2-nitrobenzyl bromide, THF, rt, 22%.

The unhalogenated and brominated phenols (**2** and **17**) were reacted with 4,5-dimethoxy-2-nitrobenzyl chloroformate in the presence of triethylamine to afford the ligands coupled to the DMNB group *via* a carbonate linker (**9** and **10**, Scheme 6).

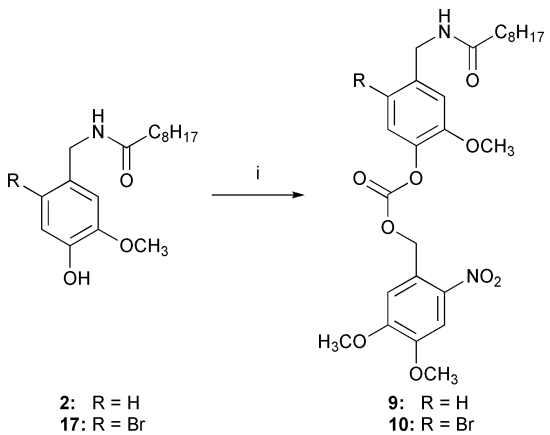

Scheme 6 Protection of the TRPV1 ligands **2** and **17** with the 4,5-dimethoxy-2-nitrobenzyl caging group *via* a carbonate linker. Reagents and conditions: R = H: i. 4,5-dimethoxy-2-nitrobenzyl chloroformate, Et_3N, CH_2Cl_2, 0 °C → rt, 100%. R = Br: i. 4,5-dimethoxy-2-nitrobenzyl chloroformate, Et_3N, CH_2Cl_2, 0 °C → rt, 92%.

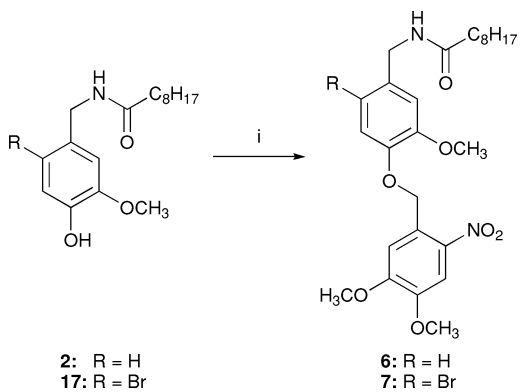

Scheme 4 Protection of the TRPV1 ligands **2** and **17** with the 4,5-dimethoxy-2-nitrobenzyl caging group. Reagents and conditions: R = H: i. ^{t}BuOK, 4,5-dimethoxy-2-nitrobenzyl bromide, THF, rt, 66%. R = Br: i. ^{t}BuOK, 4,5-dimethoxy-2-nitrobenzyl bromide, THF, rt, 53%.

All caged compounds were found to be stable in a –20 °C freezer, in the dark, for at least three months.

Laser photolysis studies

In order to determine whether photolysis of the photolabile protecting group occurred and also the nature of the products that were formed, laser photolysis studies were performed. The light source for these experiments was a frequency tripled Nd:YAG laser (Continuum Surelite) emitting 4 ns pulses with 100 mJ pulse energy at a repetition rate of 10 Hz and wavelength of 355 nm. The output of the laser was carefully attenuated to provide a pulse energy of 20 mJ for the experiments. A 3 mM solution of the compound in THF solvent was exposed to the laser radiation for durations ranging from 0–5 min and then the products analysed by ^{1}H NMR (by integration relative to an internal standard of hexamethyldisiloxane). The data for these experiments have been summarised graphically (Fig. 2A–D). The DMNB-caged compound **6** was photolysed by the laser irradiation to give the expected TRPV1 agonist (**2**) (Fig. 2A). After 5 min 61% of the total initial material comprises the uncaged product and there is approximately 4% of the caged material remaining. The DMNB carbonate-caged compound **9** was photolysed less efficiently, to give 21% of the desired TRPV1 agonist (**2**) with 23% of the caged material remaining after 5 min (Fig. 2B). The DMNB-caged compound **7** released 42% of the desired TRPV1 antagonist (**17**), upon photolysis, with 5% of the caged material remaining after 5 min (Fig. 2C). Again, the DMNB carbonate-caged compound **10** was photolysed less efficiently, with 28% of the desired TRPV1 antagonist released after 5 min and 24% of the caged material remaining (Fig. 2D).

It is interesting to note that, in all cases, the sum of the caged material and the uncaged material is less than the maximum amount of material that was present at the start of the experiment. Given that the control samples contain approximately all of the material that would be expected, loss of material simply through experimental handling seems unlikely. Therefore, it seems that an unwanted photodegradation of either the caged material or the uncaged product is occurring. To investigate whether the uncaged material was further degrading once the photolabile protecting group was removed, compounds **2** and **17** were irradiated for 4 min with a 355 nm frequency tripled Nd:YAG laser at 95 mJ power. Neither irradiation of the TRPV1 agonist **2** (*i.e.* the material that is produced by photolysis of **6** and **9**) nor the TRPV1 antagonist **17** (*i.e.* the material that is produced by photolysis of **7** and **10**) produced loss of material. These data suggest that the desired product is photostable once produced and hence there seems to be more than one photodegradation pathway for the caged material, one of which leads to the desired material and one of which leads to production of an unidentified and unwanted product. Alternatively, it may be possible for the by-products of the caging group to interact with the desired products of photolysis, leading to degradation of the material.

It is difficult to extrapolate the significance of these results to *in vitro* photolysis, as the conditions used to investigate the laser photolysis of these compounds are necessarily different from those employed when irradiating in cells. In order to make detection of the products possible, a greater quantity of material is used, and therefore photolysis for a greater length of time (than in an *in vitro* setting) is required in order to photolyse a significant proportion of the caged material. It is therefore possible that the observed photodegradation is an artefact of the conditions employed. The data do seem to indicate that more efficient photolysis is observed when the DMNB-caged compounds are employed compared to when the DMNB carbonate-caged material is photolysed. This is in accordance with a comparison made between these caging groups when photoreleasing the mitochondrial uncoupler AG10.[26] In the case of AG10, however, it emerged that despite the reduced efficiency of the DMNB carbonate-caged compound, it was significantly more soluble than the DMNB-caged material in DMSO and water, and hence is a more useful biological tool.

Photolysis in cultured trigeminal neurons

We have previously shown that photolysis of the phenacyl-caged TRPV1 agonist **3**, in dorsal root ganglion neurons, led to activation of TRPV1 receptors.[15] However, photolysis studies on **3** showed that the phenacyl group was cleaved very inefficiently and therefore **3** is not the optimal molecular probe for the study of TRPV1 receptors. Above, we have demonstrated that the DMNB-caged TRPV1 agonist **6** is photoreleased efficiently to give the expected product of nonivamide (**2**). To determine the photolysis characteristics of **6** in living cells, we performed *in vitro* photolysis experiments on trigeminal neurons in culture (Fig. 3). A subpopulation of trigeminal neurons is known to express native TRPV1 receptor channels[27] that are highly permeable to Ca^{2+} and mediate, upon agonist binding, depolarising membrane currents and transient increases in intracellular concentration of Ca^{2+} ($[Ca^{2+}]_i$).[27] Therefore, in order to detect TRPV1 channel activation induced by photolysis of the caged agonist (**6**) we performed electrophysiological recordings and $[Ca^{2+}]_i$ imaging.

Using whole-cell patch clamp recordings in voltage clamp mode, we found that, in the absence of UV light, application of the caged compound **6** (1 μM) did not produce any measurable membrane current (Fig. 3A). However, when trigeminal neurons were exposed to a brief flash of UV laser light (500 ms, 375 nm), large inward currents were observed (Fig. 3A, lower trace). On average, in 3 neurons, the peak current amplitude was 2036 ± 375 pA. These currents had a rapid onset (the mean time of current rise from 10 to 90% of the peak: 380 ± 100 ms, $n = 3$). Shorter laser flashes (10 ms) also induced membrane currents with lower peak amplitude (590 ± 120 pA; $P < 0.05$). Notably, the caged compound had to be applied at least 30 s prior to the UV flash photolysis, because shorter pre-application times failed to produce reliably significant currents (data not shown). The shape and time-course of the uncaging-induced currents were similar to these of the currents triggered in the same cells by rapid application of capsaicin (1 μM, 1 s; Fig. 3B, lower trace). On average, in 13 neurons, capsaicin-induced currents had a peak amplitude of 1610 ± 330 pA and a rise-time of 560 ± 10 ms. As expected, in cells that failed to respond to capsaicin, photolysis of the caged compound **6** also failed to induce membrane currents (data not shown). Both the responses to capsaicin, and the responses to uncaging of **6** were fully blocked by the TRPV1 antagonist capsazepine (10 μM, Fig. 3A and B, upper traces). These results were repeated in 6 cells (data not shown). These data demonstrate that the caged TRPV1 agonist **6** itself does not activate membrane currents in the absence of UV light exposure and that uncaging of the compound with

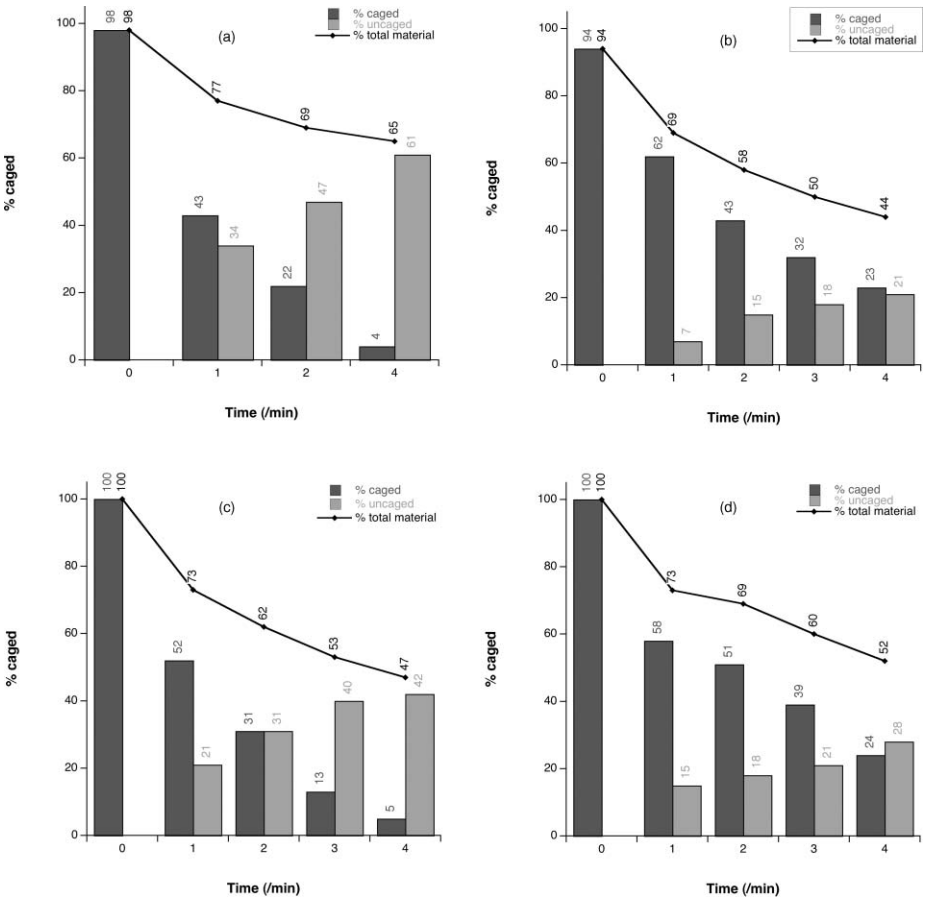

Fig. 2 (A) The photolysis profile of **6** when irradiated at 355 nm by a frequency-tripled Nd:YAG laser [(Continuum Surelite) generating ~4 ns pulses at a power of 20 mJ with a pulse repetition frequency of 10 Hz], as judged by ^{1}H NMR (observing disappearance of the doublet at δ 4.40 ppm corresponding to the caged material and the appearance of the double at δ 4.36 ppm, corresponding to the uncaged material). The dark grey bars represent the amount of caged material (**6**) present, at the time shown, expressed as a percentage of the initial amount of caged material. The light grey bars represent the amount of uncaged material (**2**) present, at the time shown, expressed as a percentage of the initial amount of caged material. The black diamonds represent the sum of the caged and the uncaged material, at the time shown, expressed as a percentage of the initial amount of caged material. A line has been used to join these points as a guide to the eye. The data point at time = 0 is taken from the control sample, which has been exposed to the same experimental procedure as the other samples, except for laser photolysis. Therefore, any photolysis observed in this sample is caused by ambient light. (B) The photolysis profile of **9** when irradiated at 355 nm by a frequency-tripled Nd:YAG laser [(Continuum Surelite) generating ~4 ns pulses at a power of 20 mJ with a pulse repetition frequency of 10 Hz], as judged by ^{1}H NMR (observing disappearance of the doublet at δ 4.41 ppm corresponding to the caged material and the appearance of the double at δ 4.34 ppm, corresponding to the uncaged material). The dark grey bars represent the amount of caged material (**9**) present, at the time shown, expressed as a percentage of the initial amount of caged material. The light grey bars represent the amount of uncaged material (**2**) present, at the time shown, expressed as a percentage of the initial amount of caged material. The black diamonds represent the sum of the caged and the uncaged material, at the time shown, expressed as a percentage of the initial amount of caged material. A line has been used to join these points as a guide to the eye. The data point at time = 0 is taken from the control sample, which has been exposed to the same experimental procedure as the other samples, except for laser photolysis. Therefore, any photolysis observed in this sample is caused by ambient light. (C) The photolysis profile of **7** when irradiated at 355 nm by a frequency-tripled Nd:YAG laser [(Continuum Surelite) generating ~4 ns pulses at a power of 20 mJ with a pulse repetition frequency of 10 Hz], as judged by ^{1}H NMR (observing disappearance of the doublet at δ 4.45 ppm corresponding to the caged material and the appearance of the double at δ 4.42 ppm, corresponding to the uncaged material). The dark grey bars represent the amount of caged material (**7**) present, at the time shown, expressed as a percentage of the initial amount of caged material. The light grey bars represent the amount of uncaged material (**17**) present, at the time shown, expressed as a percentage of the initial amount of caged material. The black diamonds represent the sum of the caged and the uncaged material, at the time shown, expressed as a percentage of the initial amount of caged material. A line has been used to join these points as a guide to the eye. The data point at time = 0 is taken from the control sample, which has been exposed to the same experimental procedure as the other samples, except for laser photolysis. Therefore, any photolysis observed in this sample is caused by ambient light. (D) The photolysis profile of **10** when irradiated at 355 nm by a frequency-tripled Nd:YAG laser [(Continuum Surelite) generating ~4 ns pulses at a power of 20 mJ with a pulse repetition frequency of 10 Hz], as judged by ^{1}H NMR (observing disappearance of the doublet at δ 4.46 ppm corresponding to the caged material and the appearance of the double at δ 4.40 ppm, corresponding to the uncaged material). The dark grey bars represent the amount of caged material (**10**) present, at the time shown, expressed as a percentage of the initial amount of caged material. The light grey bars represent the amount of uncaged material (**17**) present, at the time shown, expressed as a percentage of the initial amount of caged material. The black diamonds represent the sum of the caged and the uncaged material, at the time shown, expressed as a percentage of the initial amount of caged material. A line has been used to join these points as a guide to the eye. The data point at time = 0 is taken from the control sample, which has been exposed to the same experimental procedure as the other samples, except for laser photolysis. Therefore, any photolysis observed in this sample is caused by ambient light.

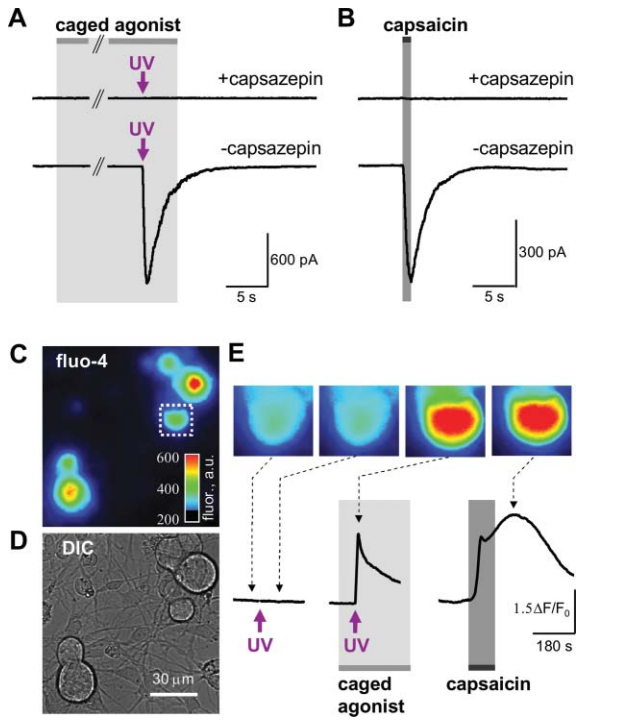

Fig. 3 Membrane currents and intracellular Ca^{2+} transients induced by TRPV1 receptor agonists in cultured trigeminal neurons. (A), Patch-clamp recordings of transmembrane current from a single cultured neuron stimulated by UV laser photolysis of caged TRPV1 agonist **6** (1 µM). The caged agonist **6** was applied through the fast perfusion system (light grey box) 30 s prior to the laser flash. Note lack of membrane current activation in response to the caged compound itself. In contrast, immediately after the UV laser flash (500 ms, violet arrow) a large membrane current is observed in the absence of the TRPV1 receptor antagonist capsazepin (lower trace) but not in the presence (10 µM) of this antagonist (upper trace). (B), Transmembrane current recorded from another cultured neuron stimulated by application of capsaicin (0.2 µM) for 1 s *via* fast perfusion system (dark grey box). The response is fully blocked by capsazepin (10 µM, upper trace). Note the similarity between membrane currents induced by capsaicin application and by photolysis of caged agonist (lower traces in A and B). (C), Pseudo-coloured image of cultured neurons loaded with a Ca^{2+}-sensitive indicator fluo-4. Dashed-line box indicates the cell shown in E. (D), Translucent image of the same field as in C obtained using differential interference contrast (DIC) technique. (E), changes in intracellular Ca^{2+} concentration in a single neuron (boxed in C). Note the lack of change in response to UV flash alone (flat trace in the left panel), as well as in response to application of the caged TRPV1 agonist in the absence of UV irradiation (light grey bar in the middle panel). In contrast, the UV flash in the presence of the caged agonist induced a large and rapid increase in $[Ca^{2+}]_i$ (middle panel), comparable in amplitude to the response to capsaicin (right panel). Four fluorescence images corresponding to four specific time points are shown above the traces.

sub-second UV flashes induces rapidly rising membrane currents. It is likely that the photoreleased compound is activating TRPV1 receptor-mediated currents, as the observed currents are similar to capsaicin-induced currents and highly sensitive to the selective TRPV1 antagonist capsazepin.[28]

In a second series of experiments, we loaded cultured trigeminal neurons with a Ca^{2+}-sensitive dye fluo-4 and monitored changes in $[Ca^{2+}]_i$ induced by photolysis of the caged agonist (**6**). Fig. 3 illustrates images of colour-coded fluo-4 fluorescence (Fig. 3C) and the translucent image of the same cells (Fig. 3D). Prior to bath application of the caged agonist **6**, we tested whether exposure to UV light alone would produce measurable changes in $[Ca^{2+}]_i$. The flat trace in Fig. 3E (left panel) demonstrates that the 50 ms UV flash had no effect on $[Ca^{2+}]_i$. This lack of effect is also illustrated by the similarity of the first two images in Fig. 3E, which were obtained before and after the UV flash. No response to UV light alone was observed in other cells in the same visual field and in 25 cells studied in similar experiments (data not shown). When we bath-applied the caged compound **6** to the same cells, no change in $[Ca^{2+}]_i$ was detected in response to the caged compound alone. However, in the presence of the caged compound the 50 ms UV flash induced a rapidly rising $[Ca^{2+}]_i$ transient (Fig. 3E, middle trace). Similar responses to uncaging were observed in approximately 50% of neurons ($n = 145$) tested in nine separate experiments (data not shown). Within 10 min of stimulation, the $[Ca^{2+}]_i$ level returned to the pre-stimulus baseline, after which cells were exposed to bath-applied capsaicin (0.2 µM, 100 s). The right panel of Fig. 3E shows the capsaicin-induced $[Ca^{2+}]_i$ rise, which had a comparable amplitude but a much slower rise time as compared to the uncaging-induced $[Ca^{2+}]_i$ transient. In three similar experiments, the same cells that responded to capsaicin also showed a response to photolysis of the caged compound (data not shown). These results support the conclusions from our electrophysiological data, demonstrating that the caged compound (**6**) alone, as well as UV light alone, have no effect on $[Ca^{2+}]_i$, that photolysis of the caged compound produces a $[Ca^{2+}]_i$ transient in capsaicin-sensitive trigeminal neurons, and that the $[Ca^{2+}]_i$ response to uncaging has a more rapid onset than that induced by bath application of capsaicin.

Taken together, our data on cultured trigeminal neurons demonstrate that the caged compound **6** is a suitable tool for studying the TRPV1 receptor with enhanced temporal and spatial control in living cells *in vitro* and, potentially, in the more intact preparations such as tissue slices or whole animal.

Initial studies on the *in vitro* photolysis of a caged TRPV1 antagonist focused on the DMNB-caged antagonist **7**, however, this compound was found to have low solubility in water or DMSO and hence was not suitable for use in *in vitro* experiments. The caged antagonist **10** was shown to be more soluble in DMSO and was therefore selected for our studies. It was first shown that application of **17** (*i.e.* the photolysis product of **10**) prior to application of capsaicin did indeed abrogate the capsaicin response, as reported by Appendino and co-workers (data not shown).[23,24] However, we were surprised to find that compound **10** was toxic to the neurons, leading to progressive irreversible cell depolarisation within 10–20 s following application. Consequently, no *in vitro* photolysis experiments were attempted with this compound. We do not think that degradation of the caging group is responsible for the observed toxicity, as the same caging group has previously been employed in caged mitochondrial uncouplers. In this instance, the caged compound was found to be biologically inactive prior to photolysis.[26] Studies to determine the root of the toxicity, and whether it is limited to compound **10** or is a feature of all caged TRPV1 antagonists of this nature, are ongoing.

Conclusion

In conclusion, we have reported a robust route for the synthesis of a set of TRPV1 agonists and antagonists and their caged derivatives. These compounds possess different physical properties and therefore will likely be applicable to different situations and experiments. We have assessed the photolysis characteristics of four of the caged compounds using a 355 nm laser and demonstrated that, in all cases, the desired TRPV1 ligand is released after photolysis. The photolysis of the caged TRPV1 agonist **6** was investigated in cultured trigeminal neurons, where it was shown to be inactive in the absence of UV irradiation, however, upon UV irradiation of this compound, fast responses consistent with activation of TRPV1 receptors were observed. This compound, used in micromolar or submicromolar concentrations enables the activation of TRPV1 *in vitro* with enhanced spatial and temporal control over standard methods of compound application. Hence this compound is likely to be a useful molecular probe for the study of TRPV1 receptors and Ca^{2+} signalling in general.

Experimental

For general experimental procedures please see the ESI.†

3-Methoxy-4-(triisopropylsilyloxy)benzonitrile (12)

To a solution of 4-hydroxy-3-methoxybenzonitrile (**11**, 10.0 g, 67.0 mmol) and imidazole (14.1 g, 210.0 mmol) in dry DMF (100 ml) at room temperature was added triisopropylsilyl chloride (16.8 g, 18.6 ml, 87.0 mmol) and the resulting solution stirred overnight. The solvent was removed *in vacuo*, and the residue purified by silica gel chromatography, eluting with petroleum ether and ethyl acetate (95 : 5), to afford 3-methoxy-4-(triisopropylsilyloxy)benzonitrile (**12**, 18.7 g, 91%) as colourless solid (found: C, 66.89; H, 9.19; N, 4.54. $C_{17}H_{27}NO_2Si$ requires C, 66.89; H, 8.91; N, 4.59); R_f 0.38 (ethyl acetate–petroleum ether, 10 : 90); mp 47–48 °C (from ethyl acetate–hexane); ν_{max} (KBr disc)/cm^{-1} 2850 (m), 2221 (s), 1594 (m), 1507 (s), 1333 (m), 1288 (s), 1160 (m), 1134 (m), 1036 (m), 990 (w), 936 (w), 900 (s), 820 (w) and 684 (m); δ_H ($CDCl_3$, 300 MHz) 7.16 (1H, dd, *J* 8.2, 2.0, C*H*–CCN), 7.07 (1H, d, *J* 2.0, C*H*–$COCH_3$), 6.90 (1H, d, *J* 8.2, C*H*–COTIPS), 3.83 (3H, s, OCH_3), 1.34–1.20 (3H, m, Si[C*H*$(CH_3)_2]_3$) and 1.09 (18H, d, *J* 7.00, Si[CH(CH_3)$_2]_3$; δ_C ($CDCl_3$, 75 MHz) 151.6, 150.5, 126.5, 121.2, 119.8, 115.3, 104.6, 56.0, 18.2 and 13.3; HRMS *m*/*z* (ES^+) [found $(M + Na)^+$ 328.1715, $C_{17}H_{27}NaNO_2Si$ requires M^+ 328.1709]; *m*/*z* (ES^+) 360 ([M + Na + MeOH]$^+$, 15), 328 ([M + Na]$^+$, 100).

3-Methoxy-4-(triisopropylsilyloxy)benzylamine (13)

A solution of 3-methoxy-4-(triisopropylsilyloxy)benzonitrile (**12**, 500 mg, 1.64 mmol) in dry diethyl ether (10 ml) was added to a stirred mixture of $LiAlH_4$ (93.2 mg, 2.46 mmol) in dry diethyl ether (40 ml). After 1 h, TLC analysis indicated that the reaction was complete and the $LiAlH_4$ was quenched with wet diethyl ether (20 ml). The solvent was removed *in vacuo* before the residue was redissolved in dichloromethane (40 ml) and filtered through Celite. The solution was evaporated *in vacuo* yielding crude 3-methoxy-4-(triisopropyloxy)benzylamine (**13**, 450 mg, crude 89%) as a yellow oil. δ_H ($CDCl_3$, 300 MHz) 6.83 (1H, d, *J* 8.0, C*H*–COTIPS), 6.82 (1H, br s, C*H*–$COCH_3$), 6.72 (1H, dd, *J* 8.0, 2.1, C*H*–CCH_2), 3.81 (3H, s, OCH_3), 3.79 (2H, s, CH_2–NH_2), 1.34–1.18 (3H, m, Si[C*H*$(CH_3)_2]_3$), 1.09 (18H, d, *J* 6.9 Si[CH(C*H*$_3)_2]_3$).

3-Methoxy-4-(triisopropylsilyloxy)-*N*-(nonanoyl)benzylamine (14)

To a solution of 3-methoxy-4-(triisopropylsilyloxy)benzylamine (**13**, 3.64 g, 11.8 mmol) in dry dichloromethane (80 ml) under nitrogen was added 4-DMAP (72.1 mg, 0.59 mmol). The resulting solution was cooled to 0 °C and dry pyridine (1.40 g, 1.43 ml, 17.7 mmol) was added dropwise. After stirring for 30 min at 0 °C, nonanoyl chloride (2.29 g, 2.34 ml, 13.0 mmol) was added dropwise. The reaction solution was allowed to warm to rt and stirred for 36 h before TLC analysis indicated that the reaction was complete. The reaction was quenched with water (100 ml) and extracted with diethyl ether (2 × 75 ml), which was washed with HCl (2 M, 75 ml) and back extracted with diethyl ether (75 ml). The ethereal layers were combined and concentrated *in vacuo* and the resulting residue was purified using silica gel column chromatography, eluting with ethyl acetate and hexane (20 : 80), to afford 3-methoxy-4-(triisopropylsilyloxy)-*N*-nonanoylbenzylamine (**14**, 4.11 g, 78%) a colourless oil. R_f 0.32 (ethyl acetate–petroleum ether, 30 : 70); ν_{max} (thin film)/cm^{-1} 3281 (m), 3073 (w), 2934 (s), 1639 (s), 1508 (s), 1465 (s), 1418 (m), 1382 (m), 1285 (s), 1234 (m), 1159 (s), 1128 (m), 1041 (m), 1016 (w), 997 (w), 884 (s), 685 (s); δ_H ($CDCl_3$, 300 MHz) 6.82 (1H, d, *J* 8.0, C*H*–COTIPS), 6.77 (1H, d, *J* 2.0, C*H*–$COCH_3$), 6.70 (1H, dd, *J* 8.0, 2.0, C*H*–CCH_2), 5.67 (1H, br s, N*H*), 4.36 (2H, d, *J* 5.6, ArCH_2NH), 3.79 (3H, s, OCH_3), 2.21 (2H, t, *J* 7.6, C(O)–CH_2–CH_2), 1.75–1.60 (2H, m, C(O)–CH_2–CH_2), 1.37–1.18 (13H, m, Si[C*H*$(CH_3)_2]_3$ and CH_2–$(CH_2)_5$–CH_3), 1.09 (18H, d, *J* 6.9 Si[CH(C*H*$_3)_2]_3$), and 0.88 (3H, t, *J* 6.7, $(CH_2)_7$–C*H*$_3$); δ_C (75 MHz; $CDCl_3$) 173.3, 151.4, 145.3, 131.8, 120.7, 120.4, 112.3, 55.9, 43.9, 37.3, 32.2, 29.7, 29.6, 26.2, 23.1, 18.3, 14.5, 13.2; HRMS *m*/*z* (ES^+) [found $(M + Na)^+$ 472.3217, $C_{26}H_{47}NaNO_3Si$ requires M^+ 472.3223]; *m*/*z* (ES^+) 472 ([M + Na]$^+$, 100).

4-Hydroxy-3-methoxy-*N*-(nonanoyl)benzylamine (2)

To a solution of 3-methoxy-4-(triisopropylsilyloxy)-*N*-nonanoylbenzyl amine (**14**, 2 g, 4.45 mmol) in dry tetrahydrofuran (50 ml) was added tetra-*N*-butylammonium fluoride (1 M solution in THF, 6.67 ml, 6.67 mmol) and the reaction solution was stirred at rt. After 4 h, HCl (1 M aqueous solution, 100 ml) and diethyl ether (100 ml) were added to the reaction solution. The aqueous layer was extracted with diethyl ether (3 × 75 ml) and the combined organic layers were washed with brine (100 ml), dried (Na_2SO_4), filtered and the solvent removed *in vacuo*. The crude product was purified by silica gel column chromatography, eluting with petroleum ether and ethyl acetate (65 : 35), to afford 4-hydroxy-3-methoxy-*N*-(nonanoyl)benzylamine (**2**, 1.1 g, 84%) as a colourless solid (found: C, 69.61; H, 9.64; N, 4.64. $C_{17}H_{27}NO_3$ requires C, 69.59; H, 9.28; N, 4.77); R_f 0.23 (ethyl acetate–petroleum ether, 50 : 50); mp 60–61 °C (from ethyl acetate–hexane) [lit.[29] mp 52 °C]; ν_{max} ($CHCl_3$)/cm^{-1} 3506 (w), 3449 (w), 3291 (s), 2924 (s), 2854 (s), 1643 (s), 1543 (m), 1519 (s), 1460 (s), 1378 (m), 1277 (m), 1254 (w), 1235 (w), 1200 (w), 1157 (w), 1122 (w), 1033 (m), 1000 (w), 851 (w), 820 (w), 704 (w); δ_H ($CDCl_3$, 400 MHz) 6.85 (1H, d, *J* 8.0, C*H*–COH), 6.79 (1H, d,

J 1.9, C*H*–COCH$_3$), 6.74 (1H, dd, *J* 8.0, 1.9, C*H*–CCH$_2$), 5.78–5.73 (2H, m, OH and NH), 4.33 (2H, d, *J* 5.7, CH_2NH), 3.86 (3H, s, OCH$_3$), 2.18 (2H, t, *J* 7.6, C(O)–CH_2–CH$_2$), 1.67–1.60 (2H, m, C(O)–CH$_2$–CH_2), 1.34–1.22 (10H, m, CH$_2$–(CH_2)$_5$–CH$_3$), 0.86 (3H, t, *J* 6.8, CH$_2$–(CH_2)$_5$–CH$_3$); δ_C (75 MHz; $CDCl_3$) 173.8, 146.3, 145.6, 130.6, 121.0, 114.9, 111.2, 56.2, 43.8, 37.1, 32.2, 29.7, 29.6, 26.2, 23.0 and 14.5; HRMS *m*/*z* (ES$^+$) [found (M + Na)$^+$ 316.1892, $C_{17}H_{27}NO_3Na$ requires M$^+$ 316.1889]; *m*/*z* (ES$^+$) 316 ([M + Na]$^+$, 100). These data are in good agreement with the literature values.[30]

6-Bromo-3-methoxy-4-(triisopropylsilyloxy)-*N*-(nonanoyl)benzylamine (15)

To 3-methoxy-4-(triisopropylsilyloxy)-*N*-nonanoylbenzylamine (**14**, 3.00 g, 6.67 mmol) in dichloromethane (500 ml), was added dropwise a solution of bromine (2.24 g, 720 µl, 14.0 mmol) in dichloromethane (200 ml), over a period of 1.5 h at –78 °C. After stirring for a further 2 h TLC analysis indicated that all starting material had been consumed. An aqueous solution of $NaHSO_3$ (100 ml, 10% w/v) was added, the resulting mixture was filtered through Celite and the solvent removed under reduced pressure. Purification by silica gel column chromatography, eluting with ethyl acetate and petroleum ether (10 : 90) yielded 6-bromo-3-methoxy-4-(triisopropylsilyloxy)-*N*-(nonanoyl)benzylamine (**15**, 2.58 g, 73%) as a colourless solid (found: C, 59.42; H, 9.02; N, 2.59. $C_{26}H_{46}BrNO_3Si$ requires C, 59.07; H, 8.77; N, 2.65); R_f 0.42 (ethyl acetate–petroleum ether, 30 : 70); mp 50–51 °C (from ethyl acetate–hexane); ν_{max} ($CHCl_3$)/cm^{-1} 3289 (s), 3065 (w), 2924 (s), 2854 (s), 1645 (s), 1542 (s), 1505 (s), 1465 (s), 1423 (m), 1380 (s), 1354 (w), 1309 (m), 1268 (s), 1237 (w), 1204 (s), 1187 (w), 1158 (m), 1042 (m), 996 (w), 972 (m), 908 (m), 884 (s), 858 (m), 727 (m), 671 (m); δ_H ($CDCl_3$, 300 MHz) 7.01 (1H, s, CH–CBr), 6.87 (1H, s, C*H*–COCH$_3$), 5.91 (1H, t, *J* 5.7, NH), 4.42 (2H, d, *J* 5.7, CH_2NH), 3.77 (3H, s, OCH$_3$), 2.18 (2H, t, *J* 7.5, C(O)–CH_2–CH$_2$), 1.68–1.57 (2H, m, C(O)–CH$_2$–CH_2), 1.32–1.16 (13H, m, Si[C*H*(CH$_3$)$_2$]$_3$ and CH$_2$–(CH_2)$_5$–CH$_3$), 1.07 (18H, d, *J* 6.9 Si[CH(CH_3)$_2$]$_3$) and 0.88 (3H, t, *J* 6.7, (CH$_2$)$_7$–CH_3); δ_C (75 MHz; $CDCl_3$) 173.3, 150.8, 146.1, 130.5, 124.4, 114.4, 113.7, 56.0, 43.9, 37.2, 32.2, 29.71, 29.65, 29.6, 26.2, 23.0, 18.3, 14.5, 13.2; HRMS *m*/*z* (CI$^+$) [found (^{81}M + H)$^+$ 530.2485, $C_{26}H_{47}{}^{81}BrNO_3Si$ requires M$^+$ 530.2488], [found (^{79}M + H)$^+$ 528.2517, $C_{26}H_{47}{}^{79}BrNO_3Si$ requires M$^+$ 528.2509]; *m*/*z* (CI$^+$) 530 ([^{81}M + H]$^+$, 40), 528 ([^{79}M + H]$^+$, 50), 486 ([^{81}M – CH(CH$_3$)$_2$]$^+$, 100), 484 ([^{79}M – CH(CH$_3$)$_2$]$^+$, 100), 448 ([M – Br]$^+$, 70), 373 ([^{81}M – Si[CH(CH_3)$_2$]$_3$ + H], 80), 371 ([^{79}M – Si[CH(CH_3)$_2$]$_3$ + H], 80).

6-Iodo-3-methoxy-4-(triisopropylsilyloxy)-*N*-(nonanoyl)benzylamine (16)

To a stirred suspension of 3-methoxy-4-(triisopropylsilyloxy)-*N*-(nonanoyl)benzylamine (**14**, 1.00 g, 2.22 mmol), sodium bicarbonate (566 mg, 6.66 mmol) and silver trifluoroacetate (490 mg, 2.22 mmol) in dichloromethane (40 ml) was added dropwise a solution of iodine (563 mg, 2.22 mmol) in dichloromethane (60 ml) over a period of 1 h at –10 °C. After the mixture had been stirred for 48 h at rt, ^{1}H NMR analysis indicated that the reaction was incomplete, therefore, silver trifluoroacetate (147 mg, 0.67 mmol) and sodium bicarbonate (170 mg, 2.01 mmol) were added to the reaction mixture. The reaction was cooled to –10 °C and iodine (169 mg, 0.67 mmol) in dichloromethane (20 ml) was added over a period of 30 min and stirred at rt for 2 h. Subsequent ^{1}H NMR analysis again indicated that the reaction was incomplete. Further sodium bicarbonate (57 mg, 0.66 mmol) and silver trifluoroacetate (49 mg, 0.22 mmol) were added, the reaction was cooled to –10 °C and iodine (56 mg, 0.22 mmol) in dichloromethane (10 ml) was added dropwise over 15 min and stirred for 2 h at rt. After this time ^{1}H NMR analysis indicated incomplete reaction so further sodium bicarbonate (114 mg, 1.22 mmol) and silver trifluoroacetate (98 mg, 0.44 mmol) were added. The reaction was cooled to –10 °C and iodine (112 mg, 0.44 mmol) in dichloromethane (20 ml) was added dropwise over a period of 30 min and the reaction stirred overnight at rt. After this time ^{1}H NMR analysis indicated full consumption of the starting material. The reaction mixture was filtered through Celite, which was washed with dichloromethane (100 ml) and concentrated *in vacuo*. The resulting residue was then purified by silica gel column chromatography, eluting with ethyl acetate and hexane (20 : 80) and the pure fractions combined and concentrated *in vacuo*. However, the resulting solid was coloured and therefore was dissolved in dichloromethane (20 ml) and washed with sodium thiosulfate solution (20 ml), which was subsequently back extracted with dichloromethane (10 ml). The organic layers were combined, dried ($MgSO_4$), filtered and to this solution charcoal was added and the suspension stirred vigorously for 1 h, before being filtered through Celite. The solution was then concentrated *in vacuo* to yield 6-iodo-3-methoxy-4-(triisopropylsilyloxy)-*N*-(nonanoyl)benzylamine (**14**, 620 mg, 49%) as a pale yellow solid (found: C, 54.48; H, 8.17; N, 2.29. $C_{26}H_{46}INO_3Si$ requires C, 54.25; H, 8.05; N, 2.43%); R_f 0.20 (ethyl acetate–hexane, 20 : 80); mp 60–62 °C (from ethyl acetate–hexane); ν_{max} (KBr disc)/cm^{-1} 3250 (w), 2934 (s), 1628 (s), 1570 (m), 1499 (s), 1270 (m), 1206 (m), 883 (w) and 669 (m); δ_H ($CDCl_3$, 300 MHz) 7.27 (1H, s, CH–CI), 6.90 (1H, s, C*H*–COCH$_3$), 5.83 (1H, t, *J* 5.6, NH), 4.40 (2H, d, *J* 5.6, CH_2NH), 3.78 (3H, s, OCH$_3$), 2.20 (2H, t, *J* 7.6, C(O)–CH_2–CH$_2$), 1.70–1.58 (2H, m, C(O)–CH$_2$–CH_2), 1.34–1.16 (13H, m, Si[C*H*(CH$_3$)$_2$]$_3$ and CH$_2$–(CH_2)$_5$–CH$_3$), 1.08 (18H, d, *J* 6.8 Si[CH(CH_3)$_2$]$_3$) and 0.88 (3H, t, *J* 6.7, (CH$_2$)$_7$–CH_3); δ_C (75 MHz; $CDCl_3$) 173.3, 151.6, 146.1, 134.0, 130.6, 114.0, 87.1, 55.8, 48.1, 37.2, 32.2, 29.71, 29.67, 29.56, 26.2, 23.0, 18.3, 14.5 and 13.2; HRMS *m*/*z* (ES$^+$) [found (M + Na)$^+$ 598.2180, $C_{26}H_{46}INaNO_3Si$ requires M$^+$ 598.2189]; *m*/*z* (ES$^+$) 598 ([M + Na]$^+$, 10), 576 ([M + H]$^+$, 90), 60 (100).

6-Bromo-4-hydroxy-3-methoxy-*N*-(nonanoyl)benzylamine (17)

To a solution of 6-bromo-3-methoxy-4-(triisopropylsilyloxy)-*N*-(nonanoyl)benzylamine (**15**, 2.0 g, 3.78 mmol) in THF (50 ml) was added tetra-*N*-butylammonium fluoride in THF (1 M, 1.48 g, 5.30 ml, 5.3 mmol) at rt and the resulting solution stirred for 3 h. TLC analysis indicated full consumption of the starting material and therefore the solution was partitioned between diethyl ether (100 ml) and aqueous HCl (1 M, 100 ml). The aqueous phase was extracted with further diethyl ether (3 × 75 ml) and the organic fractions combined, washed with brine, dried ($MgSO_4$), filtered and concentrated *in vacuo*. Purification by silica gel column chromatography eluting with ethyl acetate and petroleum ether (30 : 70) afforded 6-bromo-4-hydroxy-3-methoxy-*N*-(nonanoyl)benzylamine (**17**, 1.22 g, 86%) as a colourless solid

(found: C, 54.94; H, 7.22; N, 3.74. $C_{17}H_{26}BrNO_3$ requires C, 54.84; H, 7.04; N, 3.76%); R_f 0.51 (ethyl acetate–petroleum ether, 70 : 30); mp 94–95 °C (from ethyl acetate–hexane) [lit.[23] mp 88 °C]; ν_{max} (nujol mull)/cm^{-1} 3384 (m), 3136 (m), 2923 (s), 2854 (s), 1653 (s), 1604 (w), 1530 (m), 1502 (s), 1465 (s), 1422 (s), 1378 (m), 1365 (m), 1270 (s), 1227 (w), 1201 (m), 1183 (w), 1154 (m), 1123 (w), 1082 (w), 1040 (w), 963 (w), 871 (m), 829 (w), 723 (m), 634 (m); δ_H ($CDCl_3$, 300 MHz) 7.08 (1H, s, CH–CBr), 6.91 (1H, s, C*H*–$COCH_3$), 6.19 (1H, s, OH), 6.04 (1H, t, *J* 5.8, NH), 4.41 (2H, d, *J* 5.8, C*H*$_2$NH), 3.83 (3H, s, OCH_3), 2.19 (2H, t, *J* 7.6, C(O)–C*H*$_2$–CH_2), 1.69–1.55 (2H, m, C(O)–CH_2–C*H*$_2$), 1.33–1.20 (10H, m, CH_2–(C*H*$_2$)$_5$–CH_3) and 0.86 (3H, t, *J* 6.7, $(CH_2)_7$–C*H*$_3$); δ_C (75 MHz; $CDCl_3$) 173.8, 146.8, 146.8, 129.6, 119.1, 115.0, 113.8, 56.8, 44.3, 37.4, 32.5, 30.0, 29.9, 29.8, 26.4, 23.3, 14.8; HRMS *m*/*z* (ES$^+$) [found (^{81}M + Na)$^+$ 396.0975, $C_{17}H_{26}{}^{81}BrNNaO_3$ requires M$^+$ 396.0973], [found (^{79}M + Na)$^+$ 394.0995, $C_{17}H_{26}{}^{79}BrNNaO_3$ requires M$^+$ 394.0994]; *m*/*z* (ES$^+$) 396 ([^{81}M + Na]$^+$, 90), 394 ([^{79}M + Na]$^+$, 100).

4-Hydroxy-6-iodo-3-methoxy-*N*-(nonanoyl)benzylamine (18)

To a solution of 6-iodo-3-methoxy-4-(triisopropylsilyloxy)-*N*-(nonanoyl)benzylamine (**16**, 620 mg, 1.08 mmol) in tetrahydrofuran (10 ml) was added TBAF in tetrahydrofuran (1 M, 1.51 ml, 1.51 mmol) and the resulting solution was stirred at rt for 1 h, after which time TLC analysis showed complete consumption of the starting material. The solution was partitioned between diethyl ether (50 ml) and an aqueous solution of HCl (1 M, 50 ml). The aqueous layer was washed with further diethyl ether (20 ml) and the organic fractions combined, dried ($MgSO_4$), filtered and concentrated *in vacuo*. The resulting oil was purified using silica gel column chromatography, eluting with ethyl acetate and petroleum ether (40 : 60) to afford 4-hydroxy-6-iodo-3-methoxy-*N*-(nonanoyl)benzylamine (**18**, 298 mg, 66%) as a colourless solid (found: C, 48.78; H, 6.52; N, 3.32. $C_{17}H_{26}INO_3$ requires C, 48.70; H, 6.25; N, 3.34%); R_f 0.53 (ethyl acetate–hexane, 40 : 60); mp 106–107 °C (from ethyl acetate–hexane) [lit.[23] mp 106 °C]; ν_{max} (KBr disc)/cm^{-1} 3250 (w), 2919 (s), 2852 (w), 1653 (s), 1528 (w), 1499 (s), 1418 (w), 1265 (s), 1200 (m), 883 (w) and 632 (w); δ_H ($CDCl_3$, 300 MHz) 7.33 (1H, s, CH–CI), 6.94 (1H, s, C*H*–$COCH_3$), 5.94 (1H, t, *J* 5.8, NH), 5.84 (1H, br s, OH), 4.40 (2H, d, *J* 5.8, C*H*$_2$NH), 3.86 (3H, s, OCH_3), 2.20 (2H, t, *J* 7.6, C(O)–C*H*$_2$–CH_2), 1.69–1.57 (2H, m, C(O)–CH_2–C*H*$_2$), 1.35–1.21 (10H, m, CH_2–(C*H*$_2$)$_5$–CH_3) and 0.87 (3H, t, *J* 6.8, $(CH_2)_7$–C*H*$_3$); δ_C (75 MHz; $CDCl_3$) 173.4, 147.4, 146.2, 132.9, 125.0, 113.1, 88.2, 56.4, 48.2, 37.2, 32.2, 29.7, 29.66, 29.5, 26.1, 23.0 and 14.5; HRMS *m*/*z* (ES$^+$) [found (M + Na)$^+$ 442.0841, $C_{17}H_{26}INaNO_3$ requires M$^+$ 442.0855]; *m*/*z* (ES$^+$) 420 ([M + H]$^+$, 100), 170 (40), 60 (55).

3-Methoxy-4-(4′-methoxyacetophenone-2-oxy)-*N*-nonanoylbenzylamine (3)

To a stirred mixture of sodium hydride (13.5 mg, 0.401 mmol, 60% dispersion in mineral oil) in DMF (10 ml) was added a solution of 4-hydroxy-3-methoxy-*N*-(nonanoyl)benzylamine (**2**, 100 mg, 0.341 mmol) in DMF (10 ml) at 0 °C. The mixture was allowed to warm to rt and stirred for 1.5 h. After this time the mixture was re-cooled to 0 °C and a solution 2-bromo-4′-methoxyacetophenone (156 mg, 0.682 mmol) in DMF (10 ml) was added and the resulting mixture stirred at 0 °C for 3 h then allowed to warm to rt and stirred for a further 48 h. After this time TLC analysis indicated full consumption of the starting material and so water (5 ml) was added and the solvent removed *in vacuo*. The resulting residue was adsorbed onto silica and purified using silica gel column chromatography eluting with ethyl acetate and hexane (55 : 45) to furnish 3-methoxy-4-(4′-methoxyacetophenone-2-oxy)-*N*-nonanoylbenzylamine (**3**, 107 mg, 71%) as a white solid (found: C, 70.5; H, 7.8; N, 3.1. $C_{26}H_{35}NO_5$ requires C, 70.7; H, 8.0; N, 3.2%); R_f 0.17 (ethyl acetate–hexane, 50 : 50); mp 76–78 °C (from ethyl acetate–hexane); ν_{max} (KBr disc)/cm^{-1} 3310 (m), 2950 (m), 2870 (w), 1630 (s), 1600 (s), 1550 (w), 1510 (s), 1450 (w), 1400 (w), 1290 (s), 1210 (s), 1160 (m), 1140 (m), 1010 (w), 990 (w), 820 (w); δ_H ($CDCl_3$, 300 MHz) 8.03–7.98 (2H, m, 2 × CH–C–C(O)), 6.98–6.94 (2H, m, 2 × C*H*–$COCH_3$), 6.84 (1H, d, *J* 1.4, C*H*–$COCH_3$), 6.77–6.71 (2H, m, Ar), 5.71 (1H, t, *J* 5.6, NH), 5.28 (2H, s, O–CH_2–C(O)), 4.36 (2H, d, *J* 5.6, C*H*$_2$NH), 3.88 (3H, s, OCH_3), 3.87 (3H, s, OCH_3), 2.19 (2H, t, *J* 7.6, C(O)–C*H*$_2$–CH_2), 1.72–1.58 (2H, m, C(O)–CH_2–C*H*$_2$), 1.36–1.20 (10H, m, CH_2–(C*H*$_2$)$_5$–CH_3) and 0.87 (3H, t, *J* 6.8, $(CH_2)_7$–C*H*$_3$); δ_C (100 MHz, $CDCl_3$) 193.0, 172.9, 164.0, 149.8, 147.0, 132.6, 130.5, 127.6, 120.0, 114.4, 114.0, 112.0, 71.8, 56.0, 55.5, 43.4, 36.8, 31.8, 29.3, 29.2, 25.8, 22.6, 14.1; HRMS *m*/*z* (ES$^+$) [found (M + Na)$^+$ 464.2415, $C_{26}H_{35}NNaO_5$ requires M$^+$ 464.2413]; *m*/*z* (ES$^-$) 440 ([M – H]$^-$, 100), 212 (40).

6-Bromo-3-methoxy-4-(4′-methoxyacetophenone-2-oxy)-*N*-nonanoylbenzylamine (4)

To a suspension of sodium hydride (38.6 mg, 0.976 mmol) in DMF (ml) at 0 °C was added a solution of 6-bromo-4-hydroxy-3-methoxy-*N*-(nonanoyl)benzylamine (**17**, 300 mg, 0.806 mmol) in DMF (6 ml). The resulting mixture was stirred at 0 °C for 30 min before being warmed to rt and stirred for 1 h. After this time the mixture was cooled to 0 °C and a solution of 2-bromo-4′-methoxyacetophenone (369 mg, 1.61 mmol) in DMF (5 ml) was added. The resulting mixture was stirred for 30 min at 0 °C and then warmed to rt and stirred overnight, after which time water (20 ml) was added and the solvents removed *in vacuo*. The resulting residue was suspended in diethyl ether (30 ml) and washed with water (20 ml). The aqueous fraction was washed with further diethyl ether (2 × 30 ml). The combined organic fractions were washed with brine (20 ml), dried ($MgSO_4$), filtered and concentrated *in vacuo*. Purification using silica gel column chromatography eluting with ethyl acetate and petroleum ether (60 : 40) furnished 6-bromo-3-methoxy-4-(4′-methoxyacetophenone-2-oxy)-*N*-nonanoylbenzylamine (**4**, 140 mg, 31%) as a colourless solid; R_f 0.22 (ethyl acetate–petroleum ether, 40 : 60); mp 134–135 °C; δ_H ($CDCl_3$, 300 MHz) 8.01–7.96 (2H, m, 2 × CH–C–C(O)), 7.00–6.95 (2H, m, 2 × CH–C–C(O) and 2 × Ar), 5.86 (1H, t, *J* 5.9, NH), 5.29 (2H, s, O–CH_2–C(O)), 4.43 (2H, d, *J* 5.9, C*H*$_2$NH), 3.90 (3H, s, OCH_3), 3.87 (3H, s, OCH_3), 2.19 (2H, t, *J* 7.6, C(O)–C*H*$_2$–CH_2), 1.69–1.58 (2H, m, C(O)–CH_2–C*H*$_2$), 1.34–1.21 (10H, m, CH_2–(C*H*$_2$)$_5$–CH_3) and 0.88 (3H, t, *J* 6.8, $(CH_2)_7$–C*H*$_3$); δ_C (75 MHz; $CDCl_3$) 192.5, 173.2, 164.5, 149.5, 147.9, 131.5, 130.8, 127.8, 118.7, 114.6, 114.5, 113.9, 72.1, 56.6, 56.0, 44.0, 37.2, 32.2, 29.7, 29.5, 26.1, 23.0, 14.5.

6-Iodo-3-methoxy-4-(4′-methoxyacetophenone-2-oxy)-*N*-nonanoylbenzylamine (5)

To a stirred mixture of sodium hydride (9.6 mg, 0.286 mmol, 60% dispersion in mineral oil) in DMF (5 ml) was added slowly a solution of 4-hydroxy-6-iodo-3-methoxy-*N*-nonanoylbenzylamine (**18**, 100 mg, 0.238 mmol) in DMF (5 ml) at 0 °C. The mixture was allowed to warm to rt and stirred for 3 h. After this time the mixture was re-cooled to 0 °C and a solution 2-bromo-4′-methoxyacetophenone (109 mg, 0.477 mmol) in DMF (5 ml) was added and stirred at 0 °C for 2 h and allowed to warm to rt and stirred overnight. TLC analysis indicated that the reaction was complete, therefore the reaction mixture was partitioned between diethyl ether (20 ml) and water (20 ml). The aqueous layer was extracted with further diethyl ether (2 × 20 ml), the ethereal layers were combined and washed with brine (20 ml), dried ($MgSO_4$) and filtered. The resulting solid was purified using silica gel column chromatography, eluting with ethyl acetate and petroleum ether (20 : 80), to furnish 6-iodo-3-methoxy-4-(4′-methoxyacetophenone-2-oxy)-*N*-nonanoylbenzylamine (**5**, 44 mg, 33%) as an off white solid (found: C, 54.99; H, 6.31; N, 2.40. $C_{26}H_{34}INO_5$ requires C, 55.03; H, 6.04; N, 2.47%); R_f 0.30 (ethyl acetate–petroleum ether, 50 : 50); mp 127–128 °C (from ethyl acetate–hexane); ν_{max} (KBr disc)/cm^{-1} 3302 (s), 2918 (m), 1691 (NHC=O, s), 1648 (s), 1602 (s), 1550 (m), 1502 (m), 1380 (m), 1201 (s), 1167 (s), 1027 (w), 975 (m), 851 (w), 835 (w), 795 (w) and 576 (w); δ_H ($CDCl_3$, 300 MHz) 7.97 (2H, m, 2 × CH–C–C(O)), 7.16 (1H, s, CH–CI), 6.96 (2H, m, 2 × C*H*–$COCH_3$), 6.95 (1H, s, C*H*–$COCH_3$), 5.98 (1H, t, *J* 5.8, NH), 5.27 (2H, s, O–CH_2–C(O)), 4.38 (2H, d, *J* 5.8, CH_2NH), 3.88 (3H, s, OCH_3), 3.84 (3H, s, OCH_3), 2.20 (2H, t, *J* 7.6, C(O)–CH_2–CH_2), 1.69–1.58 (2H, m, C(O)–CH_2–CH_2), 1.35–1.21 (10H, m, CH_2–(CH_2)$_5$–CH_3) and 0.87 (3H, t, *J* 6.8, $(CH_2)_7$–CH_3); δ_C (75 MHz; $CDCl_3$) 192.5, 173.4, 164.5, 150.5, 147.8, 135.1, 130.8, 127.8, 124.9, 114.5, 114.1, 87.1, 72.1, 56.4, 56.0, 48.2, 37.1, 32.2, 29.7, 29.6, 26.1, 23.0 and 14.5; HRMS *m*/*z* (ES$^+$) [found (M + Na)$^+$ 590.1376, $C_{26}H_{34}INaNO_5$ requires M$^+$ 590.1379]; *m*/*z* (ES$^+$) 585 ([M + NH_4]$^+$, 40), 568 ([M + H]$^+$, 90), 60 (100).

3-Methoxy-4-(4,5-dimethoxy-2-nitrobenzyl)-*N*-(nonanoyl)benzylamine (6)

To a solution of 4-hydroxy-3-methoxy-*N*-(nonanoyl)benzylamine (**2**, 0.40 g, 1.36 mmol) in dry THF (25 ml) was added potassion *tert*-butoxide (0.15 g, 1.36 ml, 1 M solution in tetrahydrofuran, 1.36 mmol) and the mixture was stirred for 25 min at rt. After this time, 4,5-dimethoxy-2-nitrobenzyl bromide (0.38 g, 1.36 mmol) was added and the resulting mixture stirred for 16 h. TLC analysis indicated full consumption of the starting material, therefore the solvent was removed *in vacuo*. The residue was partitioned between water (100 ml) and ethyl acetate (100 ml) and the aqueous layer extracted with further ethyl acetate (2 × 150 ml). The combined organic fractions were dried ($MgSO_4$), filtered and concentrated *in vacuo*. The resulting solid was crystallised from dichloromethane and diethyl ether affording 3-methoxy-4-(4,5-dimethoxy-2-nitrobenzyl)-*N*-(nonanoyl)benzylamine (**6**, 0.44 g, 66%) as a yellow solid (found: C, 63.98; H, 7.30; N, 5.60. $C_{26}H_{36}N_2O_7$ requires C, 63.92; H, 7.43; N, 5.73); R_f 0.20 (ethyl acetate–petroleum ether, 50 : 50); mp 137–138 °C (from dichloromethane–diethyl ether); ν_{max} ($CHCl_3$)/cm^{-1} 3268 (m), 2925 (s), 2855 (s), 1635 (s), 1583 (w), 1543 (m), 1524 (s), 1509 (m), 1466 (s), 1387 (m), 1320 (s), 1280 (s), 1233 (s), 1198 (w), 1168 (w), 1140 (m), 1076 (m), 1035 (m), 992 (w), 872 (m), 851 (w), 820 (w), 797 (m), 756 (w), 722 (w); δ_H ($CDCl_3$, 400 MHz) 7.76 (1H, s, CH–CNO_2), 7.49 (1H, s, C*H*–$COCH_3$–$COCH_3$), 6.89 (1H, br s, C*H*–$COCH_3$) 6.87 (1H, d, *J* 8.2, C*H*–C–O–CH_2Ar), 6.78 (1H, dd, *J* 8.2, 1.9, C*H*–CCH_2–NH), 5.70 (1H, br s, NH), 5.54 (2H, s, CH_2–O), 4.39 (2H, d, *J* 5.7, CH_2–NH), 3.97 (6H, s, $COCH_3$–$COCH_3$), 3.90 (3H, s, OCH_3), 2.21 (2H, t, *J* 7.6, C(O)–CH_2–CH_2), 1.71–1.61 (2H, m, C(O)–CH_2–CH_2), 1.36–1.22 (10H, m, CH_2(CH_2)$_5$$CH_3$) and 0.88 (3H, t, *J* 6.8, CH_2CH_3); δ_C (100 MHz; $CDCl_3$) 173.0, 154.0, 150.0, 147.8, 147.0, 138.9, 132.6, 129.9, 120.2, 114.5, 111.8, 107.9, 68.5, 56.3, 56.0, 43.3, 36.9, 31.8, 29.3, 29.2, 25.8, 22.6, 14.1; HRMS *m*/*z* (ES$^+$) [found (M + Na)$^+$ 511.2402, $C_{26}H_{36}N_2O_7Na$ requires M$^+$ 511.2420]; *m*/*z* (ES$^+$) 511 ([M + Na]$^+$, 100).

6-Bromo-3-methoxy-4-(4,5-dimethoxy-2-nitrobenzyl)-*N*-(nonanoyl)benzylamine (7)

To a solution of 6-bromo-4-hydroxy-3-methoxy-*N*-(nonanoyl)-benzylamine (**17**, 0.40 g, 1.07 mmol) in THF (20 ml) was added potassium *tert*-butoxide in THF (1 M, 1.07 ml, 1.07 mmol) and the resulting solution stirred at rt for 20 min. After this time, 4,5-dimethoxy-2-nitrobenzyl bromide (0.30 g, 1.07 mmol) was added and the resulting mixture stirred for 16 h. TLC analysis showed full consumption of the starting material and therefore the solvent was removed *in vacuo*. The resulting solid was purified by silica gel column chromatography, eluting with ethyl acetate and petroleum ether (50 : 50) then ethyl acetate to afford 6-bromo-3-methoxy-4-(4,5-dimethoxy-2-nitrobenzyl)-*N*-(nonanoyl)benzylamine (**7**, 0.32 g, 53%) as a light yellow solid (found: C, 55.30; H, 6.55; N, 4.82. $C_{26}H_{35}BrN_2O_7$ requires C, 55.03; H, 6.22; N, 4.94); R_f 0.58 (methanol–dichloromethane, 5 : 95); mp 185–186 °C (from ethyl acetate); ν_{max} (nujol mull)/cm^{-1} 3274 (m), 2925 (s), 2854 (s), 1645 (s), 1547 (w), 1524 (s), 1510 (m), 1460 (s), 1411 (w), 1171 (w), 1074 (m), 1043 (w), 990 (w), 956 (w), 873 (m), 853 (w), 797 (w), 765 (w), 723 (w); δ_H ($CDCl_3$, 300 MHz) 7.78 (1H, s, CH–CNO_2), 7.46 (1H, s, C*H*–$COCH_3$–$COCH_3$), 7.09 (1H, s, CH–CBr), 7.02 (1H, br s, C*H*–$COCH_3$), 5.93 (1H, t, *J* 5.7, NH), 5.51 (2H, O–CH_2), 4.45 (2H, d, *J* 5.7, CH_2–NH), 3.98 (3H, s, OCH_3), 3.97 (3H, s, OCH_3), 3.89 (3H, s, OCH_3), 2.20 (2H, t, *J* 7.6, C(O)–CH_2–CH_2), 1.69–1.59 (2H, m, C(O)–CH_2–CH_2), 1.35–1.20 (10H, m, CH_2(CH_2)$_5$$CH_3$) and 0.87 (3H, t, *J* 6.7, CH_2CH_3); δ_C (75 MHz; $CDCl_3$) 173.1, 154.1, 149.3, 147.9, 147.6, 138.9, 131.2, 129.1, 118.4, 114.2, 113.8, 109.4, 108.0, 68.6, 56.4, 56.2, 43.6, 36.8, 31.8, 29.3, 29.1, 25.7, 22.6, 14.1; HRMS *m*/*z* (ES$^+$) [found (^{81}M + Na)$^+$ 591.1512, $C_{26}H_{35}{}^{81}BrN_2NaO_7$ requires M$^+$ 591.1505], [found (^{79}M + Na)$^+$ 589.1529, $C_{26}H_{35}{}^{79}BrN_2NaO_7$ requires M$^+$ 589.1525]; *m*/*z* (ES$^+$) 591 ([^{81}M + Na]$^+$, 80), 589 ([^{79}M + Na]$^+$, 100).

6-Bromo-3-methoxy-4-(2-nitrobenzyl)-*N*-(nonanoyl)benzylamine (8)

To a solution of 6-bromo-4-hydroxy-3-methoxy-*N*-(nonanoyl)-benzylamine (**17**, 0.3 g, 0.81 mmol) in THF (15 ml) was added potassium *tert*-butoxide in THF (1 M, 806 µl, 0.81 mmol) and the resulting solution stirred at rt for 20 min. After this time, 2-nitrobenzyl bromide (0.17 g, 0.81 mmol) was added and the

solution stirred for a further 16 h, after which time TLC analysis indicated full consumption of the starting material. Water (10 ml) was added to the solution and the solvent removed *in vacuo*. The resulting solid was re-dissolved in dichloromethane (50 ml) and washed with water (50 ml). The aqueous phase was extracted with further dichloromethane (3 × 50 ml) and the combined organic fractions dried ($MgSO_4$), filtered and concentrated *in vacuo*. The resulting solid was purified by crystallisation and re-crystallisation from ethyl acetate to afford 6-bromo-3-methoxy-4-(2-nitrobenzyl)-*N*-(nonanoyl)benzylamine (**8**, 90 mg, 22%) as a colourless solid (found: C, 56.93; H, 6.31; N, 5.49. $C_{24}H_{31}N_2O_5Br$ requires C, 56.81; H, 6.16; N, 5.52); R_f 0.52 (ethyl acetate–petroleum ether, 60 : 40); mp 146–147 °C (from ethyl acetate); ν_{max} ($CHCl_3$)/cm^{-1} 3298 (m), 2925 (s), 2854 (s), 1646 (m), 1545 (m), 1526 (m), 1509 (m), 1464 (s), 1378 (m), 1333 (m), 1307 (w), 1265 (m), 1234 (w), 1212 (m), 1191 (m), 1163 (m), 861 (w), 797 (w), 731 (m); δ_H ($CDCl_3$, 300 MHz) 8.20 (1H, dd, *J* 8.0, 1.3, CH–CNO_2), 7.93 (1H, dd, *J* 7.8, 1.1, C*H*–C–CH_2–O), 7.71 (1H, ddd, *J* 7.8, 7.7, 1.3, C*H*–CH–C–CH_2–O), 7.51 (1H, ddd, *J* 8.0, 7.7, 1.1, C*H*–CH–CNO_2), 7.06 (1H, s, CH–CBr), 7.01 (1H, s, C*H*–$COCH_3$), 5.90 (1H, t, *J* 5.9, NH), 5.52 (2H, O–CH_2), 4.45 (2H, d, *J* 5.9, CH_2–NH), 3.90 (3H, s, OCH_3), 2.20 (2H, t, *J* 7.6, C(O)–CH_2–CH_2), 1.69–1.60 (2H, m, C(O)–CH_2–CH_2), 1.35–1.21 (10H, m, CH_2(CH_2)$_5$$CH_3$) and 0.88 (3H, t, *J* 6.8, CH_2CH_3); δ_C (75 MHz; $CDCl_3$) 173.1, 149.2, 147.6, 146.7, 134.2, 133.4, 131.1, 128.5, 125.1, 118.1, 114.2, 113.6, 68.3, 56.2, 43.6, 36.8, 31.8, 29.3, 29.2, 25.7, 22.6, 14.1; HRMS *m*/*z* (ES$^+$) [found (^{81}M + Na)$^+$ 531.1285, $C_{24}H_{31}{}^{81}BrN_2NaO_5$ requires M$^+$ 531.1294], [found (^{79}M + Na)$^+$ 529.1298, $C_{24}H_{31}{}^{79}BrN_2NaO_5$ requires M$^+$ 529.1314]; *m*/*z* (ES$^+$) 531 ([^{81}M + Na]$^+$, 90), 529 ([^{79}M + Na]$^+$, 100).

4,5-Dimethoxy-2-nitrobenzyl-2′-methoxy-4′-(nonanamidomethyl)phenyl carbonate (9)

A stirred solution of 4-hydroxy-3-methoxy-*N*-nonanoylbenzylamine (**2**, 100 mg, 0.34 mmol) in dichloromethane (10 ml) was cooled to 0 °C before 4,5-dimethoxy-2-nitrobenzyl chloroformate (282 mg, 1.02 mmol) and triethylamine (0.14 ml, 1.02 mmol) were added. The resulting solution was warmed to rt and stirred for 2 h. After this time, TLC analysis indicated full consumption of starting materials. Therefore, the solvents were removed *in vacuo* and the crude purified by silica gel chromatography eluting with hexane and ethyl acetate (50 : 50) to afford 4,5-dimethoxy-2-nitrobenzyl-2′-methoxy-4′-(nonanamidomethyl)phenyl carbonate (**9**, 179 mg, 100%) as yellow solid; R_f 0.12 (ethyl acetate–hexane, 50 : 50); mp 128–130 °C (from hexane); ν_{max} ($CHCl_3$)/cm^{-1} 2924 (m), 1769 (s), 1524 (s), 1279 (s), 1221 (m), 1073 (m), 773 (s); δ_H ($CDCl_3$, 300 MHz) 7.77 (1H, s, CH–CNO_2), 7.18 (1H, s, C*H*–$COCH_3$–$COCH_3$), 7.10 (1H, d, *J* 7.9, C*H*–C–O–C(O)-O), 6.93 (1H, d, *J* 1.8, C*H*–$COCH_3$), 6.86 (1H, dd, *J* 7.9, 1.8, C*H*–C–CH_2–O), 5.76 (1H, t, *J* 5.6, NH), 5.52 (2H, O–CH_2), 5.71 (2H, O–CH_2), 4.43 (2H, d, *J* 5.6, CH_2–NH), 4.02 (3H, s, OCH_3), 3.98 (3H, s, OCH_3), 3.82 (3H, s, OCH_3), 2.21 (2H, t, *J* 7.6, C(O)–CH_2–CH_2), 1.72–1.60 (2H, m, C(O)–CH_2–CH_2), 1.35–1.21 (10H, m, CH_2(CH_2)$_5$$CH_3$) and 0.88 (3H, t, *J* 6.7, CH_2CH_3); δ_C (100 MHz; $CDCl_3$) 173.0, 153.8, 152.8, 151.2, 148.4, 139.6, 139.3, 138.1, 126.7, 122.3, 120.0, 112.4, 109.7, 108.2, 67.1, 56.6, 56.5, 56.0, 43.4, 36.8, 31.8, 29.7, 29.3, 29.2, 25.8, 22.6, 14.1; HRMS *m*/*z* (ES$^+$) [found (M + Na)$^+$ 555.2319, $C_{27}H_{36}N_2O_9Na$ requires M$^+$ 555.2325]; *m*/*z* (ES$^+$) 555 ([M + Na]$^+$, 100).

4,5-Dimethoxy-2-nitrobenzyl-5′-bromo-2′-methoxy-4′-(nonanamidomethyl)phenyl carbonate (10)

To a stirred solution of 6-bromo-4-hydroxy-3-methoxy-*N*-nonanoylbenzyl amine (**17**, 75 mg, 0.202 mmol) in CH_2Cl_2 (15 ml) was added triethylamine (0.11 ml, 0.81 mmol) at 0 °C and the resulting solution was stirred for 30 min. After this time, 4,5-dimethoxy-2-nitrobenzyl chloroformate (111 mg, 0.403 mmol) was added and the reaction solution was stirred at rt overnight. The solvent was removed *in vacuo* and the crude product was purified by silica gel column chromatography, eluting with ethyl acetate and petroleum spirits (40–60 °C) (50 : 50), to yield 4,5-dimethoxy-2-nitrobenzyl-5′-bromo-2′-methoxy-4′-(nonanamidomethyl)phenyl carbonate (**10**, 113 mg, 92%) as a colourless solid (found: C, 53.10; H, 5.90; N, 4.47. $C_{27}H_{35}BrN_2O_9$ requires C, 53.03; H, 5.77; N, 4.58); R_f 0.18 (ethyl acetate–hexane, 45 : 55); mp 143–145 °C (from hexane); ν_{max} ($CHCl_3$)/cm^{-1} 2926 (m), 1773 (m), 1524 (s), 1279 (s), 1221 (s), 1075 (m); δ_H ($CDCl_3$, 300 MHz) 7.77 (1H, s, CH–CNO_2), 7.35 (1H, s, CH–CBr), 7.15 (1H, s, C*H*–$COCH_3$–$COCH_3$), 7.09 (1H, s, C*H*–$COCH_3$) 5.92 (1H, t, *J* 6.0, NH), 5.72 (2H, O–CH_2), 4.48 (2H, d, *J* 6.0, CH_2–NH), 4.02 (3H, s, OCH_3), 3.98 (3H, s, OCH_3), 3.82 (3H, s, OCH_3), 2.21 (2H, t, *J* 7.6, C(O)–CH_2–CH_2), 1.70–1.60 (2H, m, C(O)–CH_2–CH_2), 1.35–1.22 (10H, m, CH_2(CH_2)$_5$$CH_3$) and 0.88 (3H, t, *J* 6.8, CH_2CH_3) δ_C ($CDCl_3$, 100 MHz) 173.1, 153.8, 152.4, 150.6, 148.4, 139.6, 139.5, 136.7, 126.3, 126.27, 114.9, 113.1, 109.8, 108.2, 67.3, 56.6, 56.5, 56.3, 43.6, 36.7, 31.8, 29.3, 29.1 25.7, 22.6, 14.1; HRMS *m*/*z* (ES$^+$) [found (^{81}M + Na)$^+$ 635.1403, $C_{27}H_{35}{}^{81}BrN_2NaO_9$ requires M$^+$ 635.1409], [found (^{79}M + Na)$^+$ 633.1424, $C_{27}H_{35}{}^{79}BrN_2NaO_9$ requires M$^+$ 633.1423]; *m*/*z* (ES$^+$) 635 ([^{81}M + Na]$^+$, 100), 633 ([^{79}M + Na]$^+$, 100).

General procedure for laser photolysis

A solution of caged TRPV1 agonist/antagonist in THF (3 mM) was prepared. Care was taken to minimise exposure to background UV irradiation. UV/Vis absorption spectra were obtained using a spectrophotometer (Lambda 950, Perkin Elmer) to indicate which wavelengths were most probable to evoke successful photolysis.

For photolysis experiments, aliquots (1 ml) of the solution were placed in UV transmitting quartz cuvettes (101-QS, Hellma) and irradiated with a laser source for fixed time durations. The frequency triple Nd:YAG laser source (Surelite, Continuum) provided approximately 4 ns pulses of up to 100 mJ pulse energy at a repetition rate of 10 Hz and a wavelength of 355 nm. For photolysis experiments care was taken to ensure that the laser output pulses remained consistent and further care was taken to ensure the laser spot (diameter ~4 mm) passed unclipped on cuvette walls through the lowest point possible on the solution to ensure that sufficient mixing of the solution occurred. After exposure to laser radiation the solution was analysed using ^{1}H NMR. For quantification by ^{1}H NMR, the THF from each sample was removed and 1 ml $CDCl_3$ added. A standard solution of hexamethyldisiloxane in $CDCl_3$ was added to each sample so that the ratio of sample to standard in each aliquot was 1 : 1. This ratio

was used to determine the amount of caged and uncaged material present in the photolysis samples.

Cultivation of primary trigeminal neurons

Primary cultures of trigeminal ganglion sensory neurons were obtained from Wistar rats (P9–12). Animals were anesthetised by slowly raising levels of CO_2 and killed by decapitation. Ganglia were rapidly excised and enzymatically treated and dissociated in F12 medium (Invitrogen, Gibco, Cat. No. 31765), containing 0.25 mg ml^{-1} trypsin (Sigma), 1 mg ml^{-1} collagenase (Sigma) and 0.2 mg ml^{-1} DNAse (Sigma) at 37 °C, 1400 rpm for 20 min using Thermomixer (Eppendorf). Cells were separated from debris by consecutive centrifugation and plated on poly-L-lysine-coated 35 mm Petri dishes, glass-bottomed MatTek dishes or 12 mm coverslips in F12 medium containing 10% fetal calf serum and used within 24–72 h.

Electrophysiology and UV laser photolysis

For electrophysiological experiments, cells plated on either Petri dishes or glass coverslips were used 24 h after plating. Whole-cell patch-clamp recordings (in voltage-clamp mode) were performed using HEKA EPC-10 USB amplifier (HEKA Elektronik) at the holding potential of −70 mV, and currents were recorded using the HEKA Patch Master software (HEKA Elektronik). Patch pipettes (pulled from the Harvard Apparatus GC150F-10 glass, tip resistance of 3–5 MΩ) were filled with a solution containing (mM): 130 CsCl, 5 EGTA, 0.5 $CaCl_2$, 5 $MgCl_2$, 5 K_2ATP, 0.5 NaGTP and 10 HEPES (pH adjusted to 7.2 with CsOH). Cells were superfused (1.5–2 ml min^{-1} flow rate) at room temperature (18–22 °C) with standard extracellular solution (SES) containing (in mM): 152 NaCl, 2.5 KCl, 10 glucose, 2 $CaCl_2$, 1 $MgCl_2$, 10 HEPES (pH adjusted to 7.4 with NaOH).

Solutions of the caged TRPV1 agonist (**6**) was prepared in a dark room with dim red light and kept in light-protected labware. Stock solutions of caged agonist, capsaicin and capsazepine were prepared in DMSO at 1000 × concentration, aliquoted and kept at −20 °C. On the day of experiment, aliquot was thawed and diluted in the SES. Drug application during patch-clamp recordings was performed using rapid solution exchange system (RSC-200; BioLogic Science Instruments) that allows change of perfusion milieu around the studied cell in few milliseconds.

For photolysis of caged compounds, 5–500 ms flashes of an Oxxius UV laser (Violet-375, 375 nm, 15 mW) were used. The duration and timing of the UV flashes were controlled with the Patch Master software. Membrane current recordings, drug application with rapid solution exchange system and UV laser flashes were synchronized using TTL trigger signals provided by the Patch Master software.

Calcium imaging and UV lamp photolysis

For $[Ca^{2+}]_i$ imaging experiments, cells were plated on glass-bottomed 35 mm Petri dishes (MatTek). One to three days after plating, culture medium was replaced with the SES. $[Ca^{2+}]_i$ was measured using fluorescent Ca^{2+} indicator fluo-4 (Molecular Probes). The indicator was administered as the acetoxymethyl ether (fluo-4 AM; 5 μM, 40–50 min, 23–25 °C), mixed with the nonionic detergent Pluronic F127 (0.02%; Molecular Probes, USA). Upon a 30–60 min post-incubation, cell-bearing dishes were transferred to the CellR imaging system (Olympus Europe, Hamburg, Germany). The imaging system consisted of the IX-71 inverted microscope (Olympus) equipped with a 175 W xenon burner light source, an automated filter wheel with excitation filters and an automated turret with filter cubes. The microscope frame and all optical elements were maintained at 34 °C using the temperature control incubator (Solent Scientific, Segensworth, UK). Fluorescence of fluo-4 was excited at 500 ± 5 nm and collected at 530 ± 15 nm. Images were collected in a time-lapse mode at a rate of 0.5 Hz with a CCD camera (Orca, Hamamatsu, Japan).

For photolysis of caged TRPV1 agonist, the caged compound was dissolved from the 1000× stock solution in the extracellular solution at the final concentration of 1 μM and applied to cells by bath perfusion (1–1.5 ml min^{-1} flow rate) using a peristaltic pump. Rate of bath solution exchange was estimated by imaging the dynamics of a perfusion-applied fluorescent dye, and the full exchange time was measured as 20–25 s. Caged TRPV1 agonist was photolysed by a brief (50 ms) flash of the UV light from the 175 W xenon lamp attenuated to 8% and reflected to the cells by a dichroic mirror with the 400 nm cutoff wavelength. Filter cube turret rotation for switching between the fluo-4 imaging and uncaging modes was automatically controlled by the CellR imaging software, with each rotation occurring in 4 s.

Data analysis

Electrophysiological recordings were analysed using the Patch Master (HEKA Elektronik) and Origin (Microcal) software. For analysis of Ca^{2+} imaging data, AnalySIS (Olympus Europe) and Origin software were used. Responses were quantified as the $\Delta F/F_0$ ratio, where F_0 is the background-subtracted fluo-4 fluorescence prior to stimulation, and ΔF is the difference between the current fluorescence and F_0. Plots and Figures were constructed using Origin and PowerPoint (Microsoft).

Acknowledgements

The authors would like to thank the BBSRC, EPSRC, Leverhulme Trust, the University of St Andrews and the University of Oxford for funding. MNSH thanks HEFCE and the University of Oxford for an ORS award. SJC thanks St Hugh's College, Oxford, for the provision of research support. RG and DF were supported by the Finnish Academy (grant 127150). We are grateful to the EPSRC mass spectrometry service in Swansea for some mass spectrometry data.

References

1 S. J. Conway, *Chem. Soc. Rev.*, 2008, **37**, 1530–1545.
2 A. Szallasi and P. M. Blumberg, *Pharmacol. Rev.*, 1999, **51**, 159–211.
3 P. Dasgupta and C. J. Fowler, *Br. J. Urol.*, 1997, **80**, 845–852.
4 M. J. Caterina, M. A. Schumacher, M. Tominaga, T. A. Rosen, J. D. Levine and D. Julius, *Nature*, 1997, **389**, 816–824.
5 A. Szallasi, D. N. Cortright, C. A. Blum and S. R. Eid, *Nat. Rev. Drug Discovery*, 2007, **6**, 357–372.
6 A. Szallasi and G. Appendino, *J. Med. Chem.*, 2004, **47**, 2717–2723.
7 L. Gharat and A. Szallasi, *Drug Dev. Res.*, 2007, **68**, 477–497.
8 S. M. Westaway, *J. Med. Chem.*, 2007, **50**, 2589–2596.
9 P. Gorostiza and E. Isacoff, *Mol. BioSyst.*, 2007, **3**, 686–704.
10 G. Mayer and A. Heckel, *Angew. Chem., Int. Ed.*, 2006, **45**, 4900–4921.

11 G. Dorman and G. D. Prestwich, *Trends Biotechnol.*, 2000, **18**, 64–77.
12 C. G. Bochet, *J. Chem,. Soc. Perkin Trans. 1*, 2002, 125–142.
13 B. V. Zemelman, N. Nesnas, G. A. Lee and G. Miesenbock, *Proc. Natl. Acad. Sci. U. S. A.*, 2003, **100**, 1352–1357.
14 A. R. Katritzky, Y. J. Xu, A. V. Vakulenko, A. L. Wilcox and K. R. Bley, *J. Org. Chem.*, 2003, **68**, 9100–9104.
15 J. L. Carr, K. N. Wease, M. P. Van Ryssen, S. Paterson, B. Agate, K. A. Gallagher, C. T. A. Brown, R. H. Scott and S. J. Conway, *Bioorg. Med. Chem. Lett.*, 2006, **16**, 208–212.
16 J. Zhao, T. D. Gover, S. Muralidharan, D. A. Auston, D. Weinreich and J. P. Y. Kao, *Biochemistry*, 2006, **45**, 4915–4926.
17 V. Hagen, B. Dekowski, N. Kotzur, R. Lechler, B. Wiesner, B. Briand and M. Beyermann, *Chem.–Eur. J.*, 2008, **14**, 1621–1627.
18 D. Gilbert, K. Funk, B. Dekowski, R. Lechler, S. Keller, F. Mohrlen, S. Frings and V. Hagen, *ChemBioChem*, 2007, **8**, 89–97.
19 C. S. J. Walpole, R. Wrigglesworth, S. Bevan, E. A. Campbell, A. Dray, I. F. James, M. N. Perkins, D. J. Reid and J. Winter, *J. Med. Chem.*, 1993, **36**, 2362–2372.
20 C. S. J. Walpole, R. Wrigglesworth, S. Bevan, E. A. Campbell, A. Dray, I. F. James, K. J. Masdin, M. N. Perkins and J. Winter, *J. Med. Chem.*, 1993, **36**, 2381–2389.
21 C. S. J. Walpole, R. Wrigglesworth, S. Bevan, E. A. Campbell, A. Dray, I. F. James, K. J. Masdin, M. N. Perkins and J. Winter, *J. Med. Chem.*, 1993, **36**, 2373–2380.
22 P. Wahl, C. Foged, S. Tullin and C. Thomsen, *Mol. Pharmacol.*, 2001, **59**, 9–15.
23 G. Appendino, N. Daddario, A. Minassi, S. M. Moriello, L. De Petrocellis and V. Di Marzo, *J. Med. Chem.*, 2005, **48**, 4663–4669.
24 G. Appendino, S. Harrison, L. De Petrocellis, N. Daddario, F. Bianchi, A. S. Moriello, M. Trevisani, F. Benvenuti, P. Geppetti and V. Di Marzo, *Br. J. Pharmacol.*, 2003, **139**, 1417–1424.
25 J. C. Sheehan and K. Umezawa, *J. Org. Chem.*, 1973, **38**, 3771–3774.
26 N. Avlonitis, S. Chalmers, C. McDougall, M. N. Stanton-Humphreys, C. T. A. Brown, J. G. McCarron and S. J. Conway, *Mol. BioSyst.*, 2009, **5**, 450–457.
27 M. Simonetti, A. Fabbro, M. D'Arco, M. Zweyer, A. Nistri, R. Giniatullin and E. Fabbretti, *Mol. Pain*, 2006, **2**, 11.
28 C. S. J. Walpole, S. Bevan, G. Bovermann, J. J. Boelsterli, R. Breckenridge, J. W. Davies, G. A. Hughes, I. James, L. Oberer, J. Winter and R. Wrigglesworth, *J. Med. Chem.*, 1994, **37**, 1942–1954.
29 E. K. Nelson, *J. Am. Chem. Soc.*, 1919, **41**, 2121–2130.
30 H. L. Constant, G. A. Cordell and D. P. West, *J. Nat. Prod.*, 1996, **59**, 425–426.